MANTECH Publications

International Journal of Advance Civil Engineering and Technology
Volume 1, Issue 1, January-June, 2016

Finite Element Modelling of Short Concrete Columns Reinforced with GFRP Bars

Md. Anan Morshed, Tousif Mahmood, Prof. Dr. Mahbuba Begum

Dept. of Civil Engineering

Bangladesh University of Engineering and Technology (BUET), Bangladesh

E-mail: anan.morshed@gmail.com, tousif.mahmood@gmail.com , mahbuba@ce.buet.ac.bd

Abstract

Nonlinear finite element analysis on GFRP reinforced concrete columns were performed using ABAQUS/Standard finite element code. A damage plasticity model was used to simulate the behaviour of reinforced concrete. The perfect bonding between GFRP rebars and concrete was simulated using embedded element algorithm. A static Riks formulation was implemented to trace the stable load-displacement history of GFRP reinforced concrete up to failure. The numerical model was compared with the behaviour of three GFRP reinforced columns and two steel reinforced concrete columns under concentric loading. In this paper, we will show how the model described above reliably reproduced the peak axial stress, axial deformation at the peak stress, the post-peak behaviour and the failure mode observed in the tests.

Keywords: *Glass Fiber Reinforced Polymer (GFRP), Fiber Reinforced Concrete, Finite Element (FE) Modelling And Analysis, Column Axial Load Capacity, ABAQUS*

INTRODUCTION

As columns are one of the most important structural components that carry vertical axial compressive loads, biaxial bending and moments, their performance and safety are of utmost importance. Conventionally, columns are reinforced with steel and considered strong, but when faced with some adverse environmental phenomena or when high strength is required, steel reinforcements failed to achieve what is desired. There have been extensive reports on deterioration of concrete, loss of serviceability and failure of the brittle structure due to corrosion of steel reinforcements. This corrosion problem has been a major contributor in limiting the life expectancy of the RC

structures. Various conditions like presences of chemicals and salts in the environment, freezing, thawing, and adverse coastal conditions aggravate the corrosion process, thus resulting in rapid and steady weakening of the structure's expected strength. In recent years, fiber reinforced polymers (FRP) have proven to be a great innovation in structural engineering as a means of controlling and solving the aforementioned problems.

It's a pressing need today that infrastructures are stronger, durable, sustainable, more resistant to corrosion and affordable to maintain, repair and build. With an increase in significant research efforts in developing fiber reinforced polymers as internal reinforcement in structural components, engineers can consider FRP rebars as a viable alternative to steel reinforcements. Fiber reinforced polymers (FRPs) are composites made with several components including man-made fibers that are typically embedded in a resin matrix. Fibers such as glass, carbon and aramid provide strength and stiffness, which in turn are combined with a polymer resin like polyester or epoxy. This thermosetting matrix protects the fibers and facilitates transfer of forces through shear stress. The combination of fiber and resin creates a material with attributes superior to either of the components, and it is critical in the performance of the composites material. Composites exhibit strength that is 5 TIMES stronger than steel at ¼th the weight, and offers corrosion resistance, and many other benefits. Other advantages include high strength and stiffness-to-weight ratios, a high degree of chemical inertness, controllable thermal expansion, damping characteristics, and electromagnetic neutrality.

Extensive experimental research have been conducted by research groups on the behaviour of GFRP rebars used as internal reinforcement for beams, slabs and pavements [1,2,3] . These efforts have contributed greatly in improving our analysis and design of concrete structures reinforced with FRP bars in flexure and shear. On the other hand, the behaviour of GFRP RC compression members is less defined. Previous experiments carried out by Kobayashi [4], De Luca et al. [5], Tobbi et al. [6], Choo et al., Deitz et al. etc. studied the behaviour of FRP reinforced columns. Despite the availability of a considerable amount of experimental data for predicting the behaviour of GFRP reinforced concrete columns, a complete 3-D finite element model for

understanding the influence of various parameters, such as characteristic concrete compressive strength, reinforcement ratios and tie spacing, is somewhat lacking. To fill this gap,we have made an attempt to develop a complete 3-D finite element model of GFRP reinforced concrete short columns.

OBJECTIVES AND SCOPE OF THE STUDY

The objective of this study is to develop a complete 3D finite-element model that can be applied for short concrete columns with various material properties reinforced with GFRP bars subjected to concentric loading conditions. The model is to be capable of reproducing the full behavioural history, including the peak and post peak capacities, and the failure mode caused by buckling of the reinforcement and/or crushing of the concrete with respect to the experimental database available in the literature. The numerical simulation of GFRP RC columns is performed using ABAQUS/Standard finite element package. The finite element model incorporates the nonlinear material behaviour of concrete, bilinear stress-strain curve of steel and linear elastic behaviour of GFRP rebars. The nonlinear behaviour of concrete in the RC columns is represented by damage plasticity model. A static Riks solution strategy is used to trace a stable post-peak response of the reinforced system.

REFERENCE TEST SPECIMENS

Experimental results of 5 specimens, representing FRP-reinforced concrete columns and steel reinforced concrete columns are used to validate the numerical results. To validate the model, simulations are conducted for axially loaded square test specimens of Tobbi et al. 2012. The cross section used is 350×350 mm for 1400 mm length square columns of 33 MPa concrete. Detailed descriptions of the test specimens are provided in the following section.

The column sets tested includes five square specimens which are modelled for finite element analysis. The lists of these specimens, along with their material properties, are given in Table 1 and shown in Figure 1. These specimens had square cross sections of 350 mm X 350 mm with a height of 1400 mm. The first two specimens were reinforced with steel rebars and the latter three with glass fiber reinforced polymer (GFRP) bars. To provide lateral ties, steel ties are used in the steel reinforced columns and GFRP ties are used in GFRP reinforced columns.

The steel RC column have similar areas of longitudinal reinforcement, consisting of eight 16 mm diameter bars. In the case of the GFRP-reinforced column, 19.1 mm and 15.9 mm diameter rebars [7] were used. No.13 GFRP bars spaced at 120 mm (4.72 in) were used as ties. For the steel-reinforced columns, M10 (11.3 mm diameter) ties were used, spaced at 120 mm (4.72 in.) and 330 mm (13 in.). Figure-1 also shows the GFRP reinforcement layouts. The cross-section layout was identical for all specimens.

FINITE ELEMENT MODELLING

I. Element Types

8-noded solid 3D elements (C3D8R) were used to model the concrete. Two node linear 3D truss elements (T3D2) were used to model the reinforcement steel and GFRP rebars.

The C3D8R element selected to model the concrete of the reinforced concrete column is an eight-node reduced integration brick element with three translational degrees of

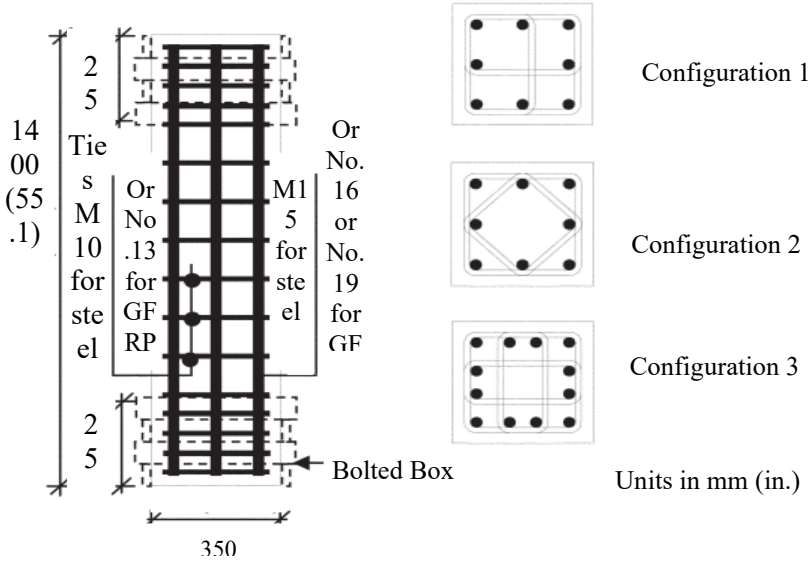

Figure 1 Reference Test Specimen Columns [6]

Specimen Designation	Bar Type	Diameter of Bar(mm)	Area of Bar (mm^2)	Tie Spacing (mm)	E_f GPa (ksi)	f_{fu} MPa (ksi)	$\in_{f\%}$
C-S-1-120	Steel	16	200	120	200(29000)	f_y = 460	$\in_y$=0.2
C-S-1-330	Steel	16	200	120	200(29000)	f_y = 460	$\in_y$=0.2
C-G-1-120	GFRP	19.1	284	120	47.6(6902)	728(106)	1.53
C-G-2-120	GFRP	19.1	284	120	47.6(6902)	728(106)	1.53
C-G-3-120	GFRP	15.9	199	120	47.6(6902)	751(109)	1.56

Table 1- Material Properties of Test Columns

freedom at each node [8, 9].

T3D2 are three dimensional truss element having two degrees of freedom. A 2-node straight truss element, which uses linear interpolation for position and displacement, has a constant stress [8,9]. The cross-sectional area associated with the truss element is defined as part of the section definition. Truss elements have no initial stiffness to resist loading perpendicular to their axis.

II. Modelling of GFRP

The embedded element technique can be used to model rebar reinforcement. If a node of an embedded element lies within a host element, the translational degrees of freedom at the node are eliminated and the node becomes an "embedded node." The translational degrees of freedom of the embedded node are constrained to the interpolated values of the corresponding degrees of freedom of the host element. Embedded elements are allowed to have rotational degrees of freedom, but these rotations are not constrained by the embedding [10].

III.Mesh Description

The mesh configuration for the full FRP confined concrete column model is shown in Figure 2. The analysis was performed using 58.33 x 58.33 x 56mm rectangular block to optimize the mesh in order to produce proper representation of the rupture of concrete cover, concrete core and GFRP rebars and properly simulate the compressive behaviour and minimize the computational time.

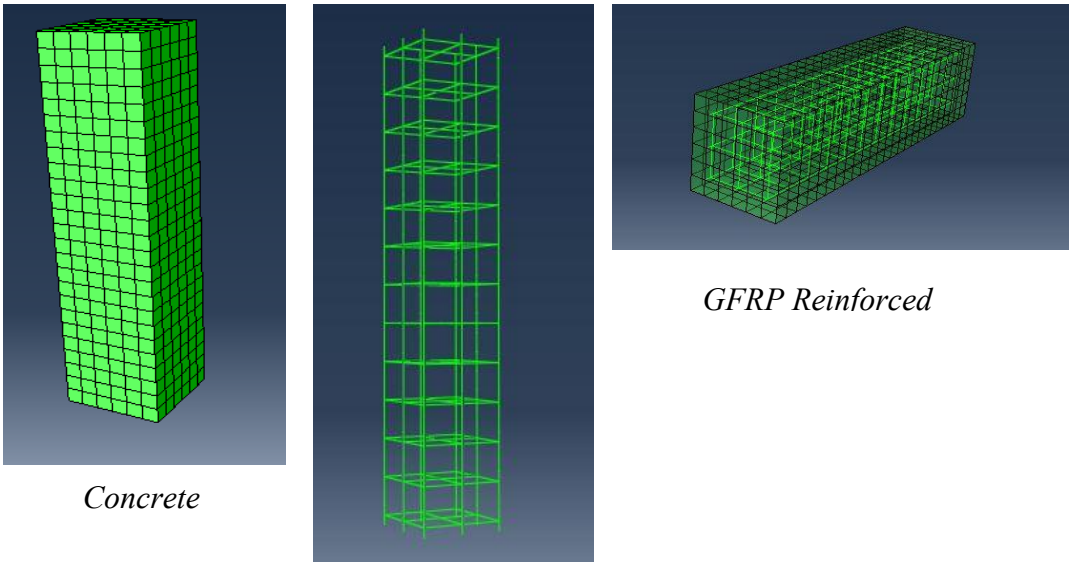

Concrete

Reinforcement

GFRP Reinforced

Figure- 2

IV. Load application and boundary conditions

In the experiment, to ensure that failure would occur in the instrumented region, the tapered ends of each specimen were further confined with bolted boxes made from 13 mm (0.5 in.) thick steel plates [6] which was not simulated in the FE model. Uniaxial compressive load is applied in the model. The load was applied using displacement control technique on the top surface of the column. The base of the column was fixed in all directions.

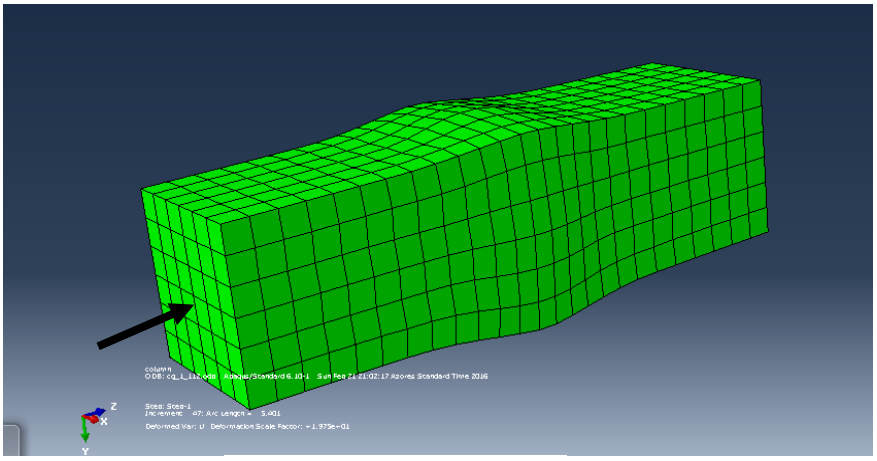

Figure- 3

V. Material Properties

The damage plasticity model in ABAQUS was used to simulate the concrete material behaviour in the RC columns. The model is a continuum, plasticity-based damage model for concrete (Lubliner et al. [16]) that is capable of predicting both compressive and tensile behaviour of the concrete material under low confining pressures. The model was verified (Begum et al. [17]) against published tri-axial compressive test results for concrete cylinders under different levels of confinement. The damage plasticity model uses a non-associated plastic flow rule to describe the plastic strain increments. The dilation angle for concrete is defined under this option to identify the plastic strain direction relative to the gradient of the yield surface. In this study, a value of 15 degrees is defined for the dilation angle of concrete.

The effective stress–plastic strain function is described through a stress–strain function (compression hardening function) in uniaxial compression using the model proposed by Carriera and Chu (1985). A general form of serpentine curve, as given by the following equations [11] is used to represent the complete stress-strain relationship of unconfined concrete

$$\frac{f_c}{f'_c} = \frac{\beta(\frac{\varepsilon}{\varepsilon'_c})}{\beta-1+(\frac{\varepsilon}{\varepsilon'_c})^{\beta}} \quad (1)$$

$$\beta = \frac{1}{1-(\frac{f'_c}{\varepsilon'_c E_{it}})} \quad (2)$$

Where, β is a material parameter which depends on the shape of the stress- strain diagram. The value of β = 3 is used in this thesis which is proposed by Tulin and Grestle [13].A stress-strain relationship curve of concrete is plotted using the above equations and this curve is shown in Figure 4 (a). Figure 4 (b) shows axial stress versus plastic strain curve for compression hardening of concrete.

$$\varepsilon'_c = (0.2\, f_{cu} + 13.06)x10^{-4} \quad (3)$$

(Almusallam & Alsayed, 1995)

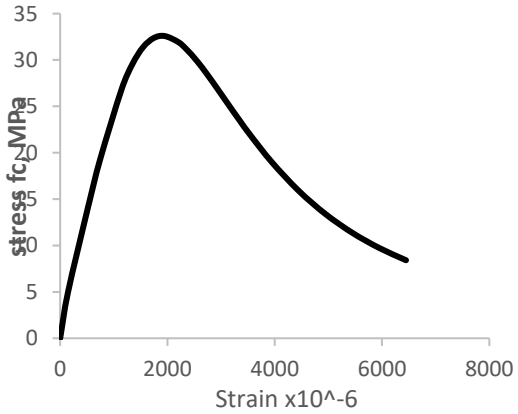

Figure 4(a)

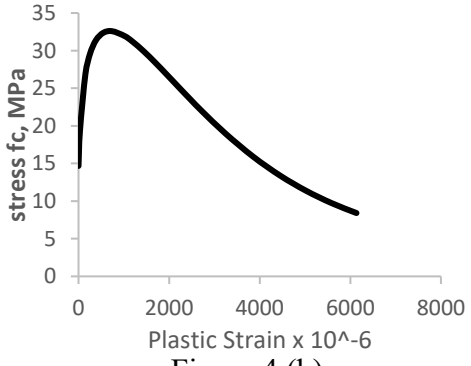

Figure 4 (b)

A same form of serpentine curve is used shown in Figure 5 (a) and (b) for the average stress-strain diagram and stress-inelastic strain diagram of reinforced concrete in tension [12], f't is taken as 10% of f'c [18].

$$\frac{f_t}{f'_t} = \frac{\beta(\frac{\varepsilon}{\varepsilon'_t})}{\beta-1+\left(\frac{\varepsilon}{\varepsilon'_t}\right)^{\beta}} \quad (4)$$

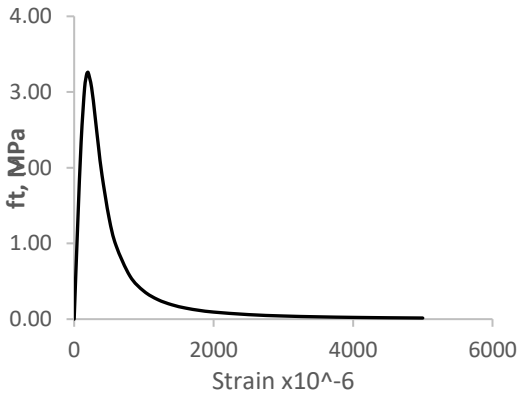

Figure 5(a)

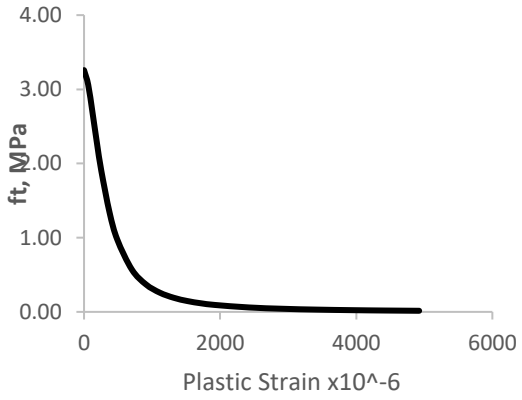

Figure 5(b)

The GFRP rebars have notable mechanical properties in comparison to steel, such as high tensile strength, corrosion resistance, and light weight. GFRP rebars that were used had 728 MPa and 751 MPa tensile strength. However, FRP rebars have significant lower compressive strength than their tensile strength [6, 15]. Moreover, there are no standards for axial compression tests of FRP bars due to their different modes of failure such as rebars buckling, and local microbuckling of individual fibers. Kobayashi and Fujisaki suggested contribution of GFRP rebars in compression to be 30-40 % of its tensile strength.

Longitudinal and transverse GFRP reinforcement behaviour in the model was defined using a linear elastic stress-strain relation with a Poisson's ratio of 0.23 [7].

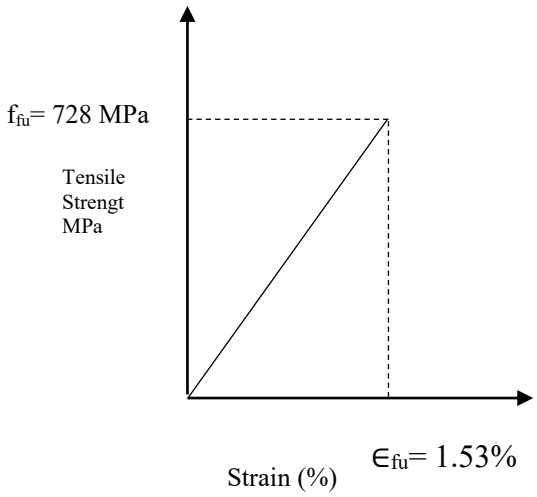

Figure 6 Elastic stress strain curve of GFRP used

VI. Solution Strategy

The solution strategy is based on the Riks method. In simple cases linear eigenvalue analysis may be sufficient for design evaluation; but if there is a concern about material nonlinearity, geometric nonlinearity prior to buckling, or unstable post buckling response, a load-deflection (Riks) analysis must be performed to investigate the problem further. The Riks method is generally used to predict unstable, geometrically nonlinear collapse of a structure.

- Can include nonlinear materials and boundary conditions.
- Often follows an eigenvalue buckling analysis to provide complete information about a structure's collapse, and
- Can be used to speed convergence of ill-conditioned or snap-through problems that do not exhibit instability.

The Riks method uses the load magnitude as an additional unknown; it solves simultaneously for loads and displacements [8].

PERFORMANCE OF FE MODEL

Ultimate stress and peak strain behaviour

The values of numerical and reference

experimental peak loads and peak strains, their ratios for the five validated columns of 33 MPa concrete strength are presented in the Table 2. The axial peak stress and peak-strain of these columns obtained from the numerical analysis matched very well with the corresponding experimental results.

Table 2- Comparison of Experimental and Numerical Results

Specimen Designation	Peak Axial stress (MPa)		$\sigma_{exp} / \sigma_{num}$	Peak Axial Strain		$\in_{exp} / \in_{num}$
	Exp	Num		Exp	Num	
C-S-1-120	44.16	37.48	1.18	4848	2952	1.64
C-S-1-330	31.18	36.42	0.86	1818	2895	0.63
C-G-1-120	40.30	33.98	1.19	4761	2946	1.62
C-G-2-120	41.47	34.09	1.22	7142	2899	2.46
C-G-3-120	44.51	41.13	1.08	9411	2949	3.19
Mean SD			1.10 0.14			1.91 0.97

The mean value of the experimental-to-numerical peak load ratio, σ exp / σ num is 1.10, with a standard deviation of 0.14. Whereas, the mean $\in$ exp / $\in$ numis 1.91 with a standard deviation of 0.97.

The numerical analysis results of the model are found to be in agreement with the experimental results in the pre-peak region. However, after the ultimate stress the strains obtained from this model are found to be lesser than those obtained experimentally.

This difference is due to some idealization done in the model. In the reference test specimen, 255 mm bolted box made of 13 mm thick steel plates were used at both ends with a thin layer of rubber capping. However, the FE model was not strengthened at the ends that prompted this reduced peak stress and early peak strain.

Figure 7 shows the performance of FE model in predicting the axial stress versus strain response for the specimens subjected to pure axial loading. For all specimens, general initial behaviour is identical to the experimental behaviour.

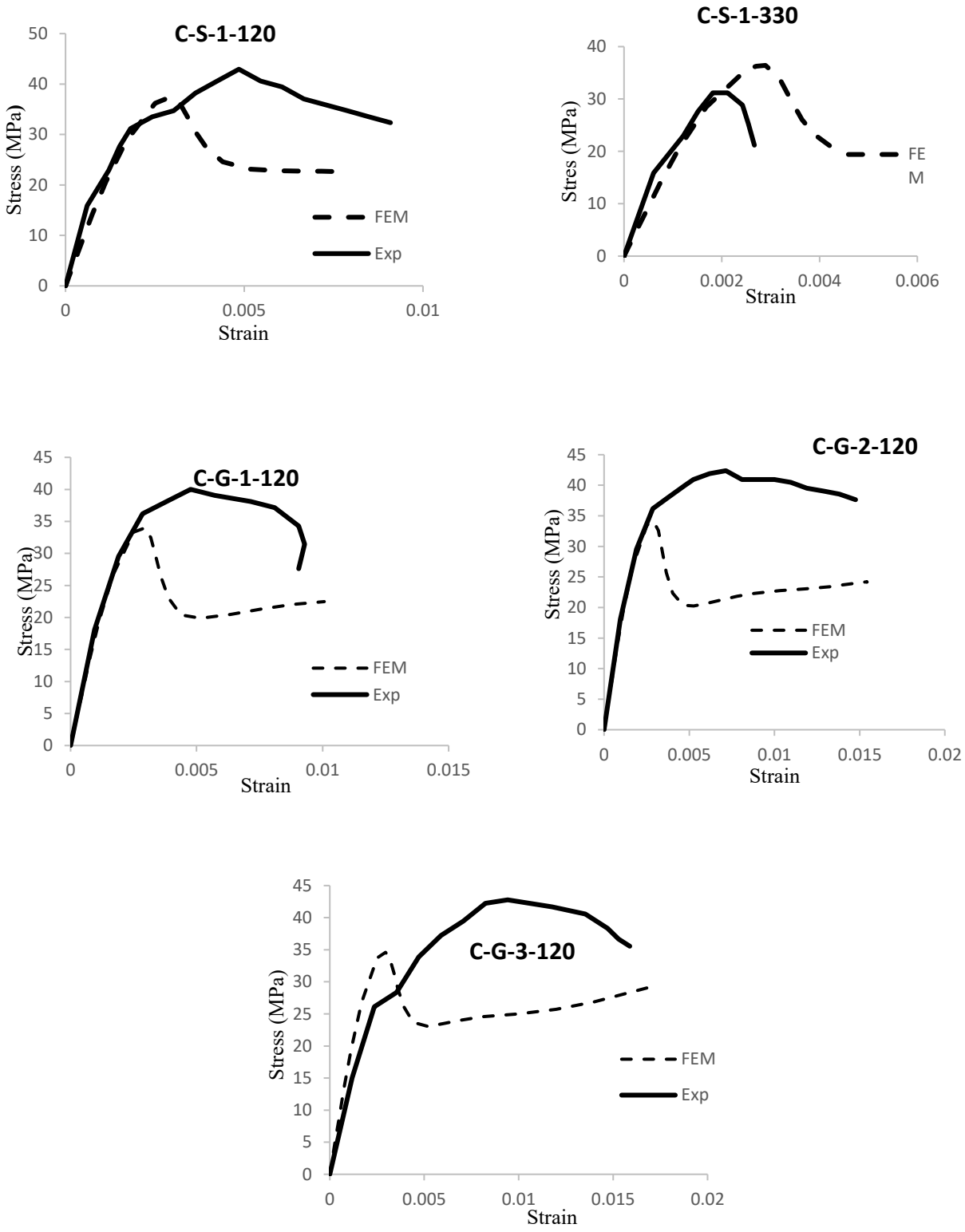

Figure 7 Numerical and Experimental Stress Versus Strain Behavior for Concentrically Loaded GFRP and Steel Reinforced Columns

Failure mode

The failure in all the GFRP reinforced specimens observed in the numerical analysis is due to the concrete core crushing and buckling of the rebars simultaneously. Similar behaviour was observed in the experiments.

Figure 8 shows the failure modes for a typical concentrically loaded specimen, observed in the numerical analysis. In all cases the failure mode matched well with that observed in the experiments [6]

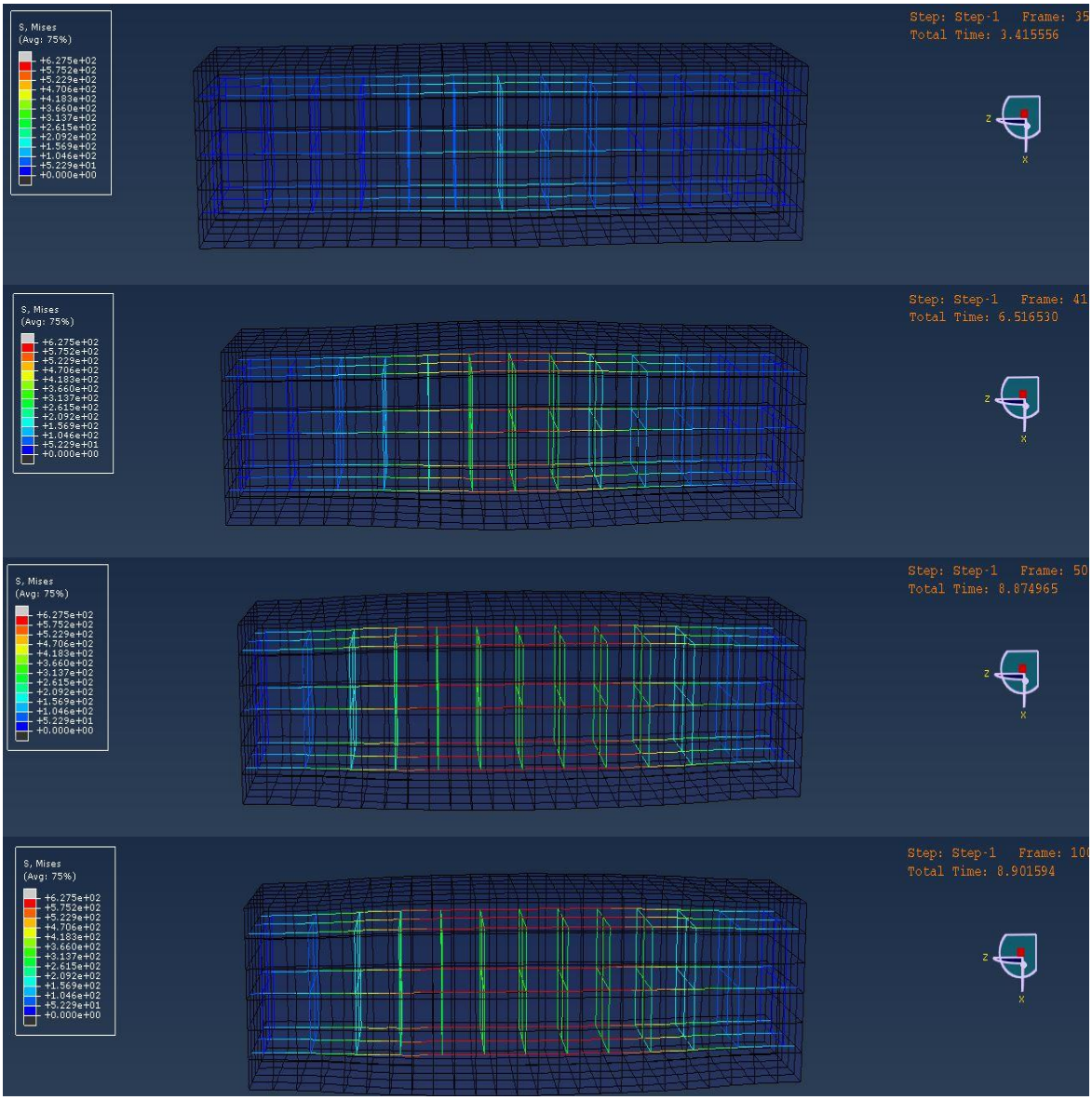

Figure 8 Behaviour of GFRP Rebars in Compression and Failure by Buckling at Different Load Stages

CONCLUSIONS

Nonlinear 3D finite element models have been developed using ABAQUS finite element software code to investigate the compressive behaviour of GFRP reinforced concrete square columns. A static, Riks solution strategy was implemented in the numerical model to trace a stable peak response in the load-deformation curve. The concrete material in the reinforced column was modelled using the damage plasticity model available in ABAQUS. The GFRP rebar was simulated using embedded element algorithms: the translational degrees of freedom of the embedded node are constrained to the interpolated values of the corresponding degrees of freedom of the host element. To investigate the performance of this FEM model, simulations were conducted for FRP reinforced concrete column test, reported in the literature. The reinforced square columns 350 x 350 x 1400 mm with normal strength concrete of 33 MPa were used. The loading condition was limited to only concentric loading. The model was found capable of predicting the peak load and post-peak behaviour quite reliably. No end strengthening was introduced in the model. This caused the deviation in the FE model results from the experimental ones.

The model can further be improved by including the steel plate bolted box for end strengthening.

For future research, effect of different parameters on the ultimate axial load capacity, such as concrete compressive strength, reinforcement ratio, tie spacing, tie configuration, geometric properties, eccentric loading, etc. can be studied.

REFERENCES

I. ACI Committee 440. Guide for the design and construction of structural concrete reinforced with FRP bars, 440.1R-06. American Concrete Institute, Farmington Hills, MI (2006)

II. Canadian Standards Association, 2002, “Design and Construction of Building Components with Fiber-Reinforced Polymers (CAN/CSA S806- 02),” Canadian Standards Association, Mississauga, ON, Canada, 177 pp.

III. Benmokrane, B. and Rahman, H. (1998). “Durability Of Fiber-Reinforced Polymer (FRP) composite for construction”, Proceedings of the First International Conference on

Durability of Composites for Construction, Sherbrooke, Quebec, Canada, Aug. 5-7, 692 .

IV. K. Kobayashi and T. Fujisaki, "Compressive behavior of FRP reinforcement in non-prestressed concrete members," in NonMetallic (FRP) Reinforcement for Concrete Structures: Proceedings of the Second International RILEM, CRC Press, 1995.

V. A. De Luca, F. Matta, and A. Nanni. Structural response of full-scale reinforced concretecolumns with internal FRP reinforcement under compressive load. 9th International Symposium on Fiber Reinforced Polymer Reinforcement for Concrete Structures(FRPRCS-9), ed. D. Oehlers, M. Griffith, and R. Seracino, July 13–15, 2009, Sydney,Australia, CD-ROM, 4 (2010).

VI. H. Tobbi, A. S. Farghali, and B. Benmokrane. Concrete columns reinforced longitudinallyand transversally with glass FRP bars. ACI Structural Journal 109 (4): 1–8 (2012).

VII. Pultrall Inc, 2009, "V-ROD Composite Reinforcing Rods Technical Data Sheet," Thetford Mines, Canada, www.pultrall.com

VIII. Abaqus 6.14 Analysis User's Guide

IX. Abaqus 6.14 Verification Guide

X. Abaqus 6.14 Keywords Reference Guide

XI. Carriera, D. J. and Chu, K.M. (1985). "Stress-strain relationship for plain concrete incompression." ACI Structural Journal, 82(6), 797-804.

XII. Carreira. D.J. Chu, Kuang-Han, Stress-strain relationship for reinforced concrete in tension, ACI. J. 84(1986)21-28.

XIII. Tulin, L. G. and Grestle, K.H.(1964). "Discussion of the equation for the stress-strain curve of the concrete." ACI Structural Journal, 61(9), 1236-1238.

XIV. C. C. Choo, I. E. Harik, and H. Gesund. Minimum reinforcement ratio for fiber reinforcedpolymer reinforced concrete rectangular

columns. ACI Structural Journal 103 (3): 460–466 (2006)

XV. D. H. Deitz, I. E. Hark, and H. Gesund. Physical properties of glass fiber reinforcedpolymer rebars in compression. Journal of Composites for Construction 7 (4): 363–366 (2003).

XVI. Lubliner, J., Oliver, J., Oller, S. and Onate, E. (1989). “A Plastic-Damage Model for Concrete.” InternationalJournal of Solids and Structures, 25 (3), 229-326.

XVII. Begum. M.,Robert G. Driver.,Alaa E. Elwi., (2007) Finite-Element Modeling of PartiallyEncased CompositeColumns Using the Dynamic Explicit Method

XVIII. Marzouk, H., and Z. W. Chen. "Fracture energy and tension properties of high-strength concrete." Journal of Materials in Civil Engineering 7.2 (1995): 108-116.